

NASA's PACE Ocean Color Instrument Thermal Design Evolution: from Goddard's Instrument Design Lab Through Flight Development

Kan Yang[1], Deepak Patel[2], and Wes Ousley[3]
NASA Goddard Space Flight Center, Greenbelt, MD, 20771

NASA's Plankton, Aerosol, Cloud, ocean Ecosystem (PACE) mission, set to launch in 2024, seeks to provide data continuity for the ocean color, aerosol and cloud measurements acquired by NASA's on-orbit Earth Science observatories since the 1990s. It will accomplish this through its Ocean Color Instrument (OCI), an optical spectrometer being developed for hyper-spectral measurements in the ultraviolet-to-near-infrared band between 340 nm and 2260 nm. Although OCI's instrument architecture will provide greater insight and resolution than its predecessors in this wavelength range, the engineering required to achieve this also poses a greater challenge. In thermal engineering, this translates to a more complex thermal control approach to address high heat dissipations, stringent stabilities, the volume of heat that requires transport, and changing thermal environments due to tilting of the entire instrument ±20° twice per orbit. This current work explores how the PACE OCI instrument design has evolved from its initial conception in NASA Goddard's Instrument Design Laboratory (IDL) to the current iteration of its flight design. The IDL studies explored three separate instrument configurations and two spatial resolutions per configuration, which were then down selected to a single instrument type and spatial resolution for flight instrument development. OCI subsequently went through major project milestones, including Preliminary Design Review (PDR), Critical Design Review (CDR), Pre-Environmental Review (PER) and Pre-Ship Review (PSR), with significant design updates along the way. This paper aims to provide a comprehensive account of OCI's thermal control architecture evolution and the engineering drivers that have shaped it, with the goal of identifying trends spanning the full instrument development timeline to inform and advance future instrument thermal designs.

Nomenclature

AOB	=	Aft Optics Bench
BSS	=	Blanket Support Structure
CCD	=	Charge Coupled Device
CCHP	=	Constant Conductance Heat Pipe
CDR	=	Critical Design Review
CSA	=	Collimator Slit Assembly
DAU	=	Data Acquisition Unit
EMI	=	Electromagnetic Interference Testing
ETU	=	Engineering Test Unit
GEVS	=	General Environmental Verification Standard
GSFC	=	NASA Goddard Space Flight Center
HAM	=	Half-Angle Mirror
HSP	=	Hyper-Spectral Pushbroom
HSS	=	Hyper-Spectral Scanner

[1] Team Lead, Instrument Design Laboratory, NASA/GSFC, Code 550.
[2] PACE OCI Thermal Product Design Lead and Associate Branch Head, Thermal Engineering Branch, NASA/GSFC, Code 545.
[3] PACE OCI Deputy Thermal Product Design Lead, Vertex Aerospace.

FEE = Front End Electronics
FOV = Field of View
FPA = Focal Plane Assembly
ICDU = Instrument Command and Data Unit
IDL = Instrument Design Laboratory
m, nm = Meter, nanometer
λ = Wavelength
LHP = Loop Heat Pipe
LTAN = Local Time of the Ascending Node
MBS = Multi-Band Scanner
MCE = Mechanism Control Electronics
MCR = Mission Concept Review
MEB = Main Electronics Box
MLI = Multi-Layer Insulation
OB, OM = Optical Bench, Optical Module
OCI = Ocean Color Instrument
PACE = NASA's Plankton, Aerosol, Cloud, ocean Ecosystem mission
PDR = Preliminary Design Review
PER = Pre-Environmental Review
PID = Proportional-Integral-Derivative control
PSR = Pre-Ship Review
RTA = Rotating Telescope Assembly
S/C = Spacecraft
SCA = Solar Calibration Assembly
SDA = SWIR Detection Assembly
SPCA = SDA Pulse Calibration Assembly
SRR = System Requirements Review
STOp = Structural, Thermal, Optical analysis
SWIR = Short-Wave Infrared
TCS = Thermal Control Subsystem
TDI = Time-Delay Integration
TEC = Thermoelectric Cooler
TV/TB = Thermal Vacuum/Thermal Balance
UVVIS = Ultraviolet-to-Visible, sometimes referred to as the "Blue" channel
VISNIR = Visible-to-Near-Infrared, sometimes referred to as the "Red" channel
W = Watt

I. Introduction

THE Plankton, Aerosol, Cloud, ocean Ecosystem (PACE) Mission is NASA's next major observatory to monitor the health of Earth's living ocean and climate and ensure data continuity on critical metrics for ocean color, aerosols, and clouds. It builds on both the repository of scientific data and prior design heritage from instruments such as the Sea-Viewing Wide Field-of-View Sensor (SeaWiFS) [1] on the OrbView-2 Satellite, the Moderate Resolution Imaging Spectroradiometer (MODIS) [2] on the Terra and Aqua satellites, and the Visible Infrared Imaging Radiometer Suite (VIIRS) [3] on Suomi NPP, to answer such essential questions as: what are the long-term changes in aerosol and cloud properties and how are they correlated with variations in climate? How is the concentration and composition of organisms in our ocean ecosystems changing, and how do they affect our food webs? What materials are exchanged between the land and ocean, and how do they affect life on our coasts as well as peoples' health and welfare?

The Ocean Color Instrument (OCI) is the primary instrument on PACE. OCI is an advanced optical spectrometer that will enable higher resolution measurement of Earth's radiance spanning the near-infrared to ultraviolet portions of the electromagnetic spectrum. OCI uses gratings for spectral light dispersion and conducts hyper-spectral measurements via separate Ultraviolet-to-Visible (UVVIS, 340-605 nm) and Visible-to-Near-Infrared (VISNIR, 600 – 890 nm) Focal Plane Assemblies (FPA). The "blue" UVVIS channel enables measurements of aerosols and microscopic marine algae, while the "red" VISNIR channel allows for studies of phytoplankton health and coastal

biology. Spectrally filtered Short Wave Infrared (SWIR) detectors in discrete bands between 940 nm to 2260 nm allow for determination of the clarity of the atmosphere over the ocean and provide information on the distribution and characteristics of clouds, enabling measurements of the near-surface concentration of chlorophyll as well as the understanding of the balance of energy that enters and leaves the climate system, helping to drive down uncertainties in models to predict future climate change. The following sections will focus on the evolution of the engineering design on the OCI instrument since 2015, with special focus on thermal design, and its eventual integration and testing on its journey to flight.

II. Ocean Color Instrument Design Trades in the Instrument Design Laboratory

Early concept studies of the OCI instrument were undertaken at NASA Goddard Space Flight Center's (GSFC) Instrument Design Laboratory (IDL). Through separate week-long sessions each employing a team of engineers in a concurrent and collaborative rapid design process, the IDL performed trade studies on three OCI instrument configurations: a Multi-Band Scanner (MBS), a Hyper-Spectral Scanner (HSS), and a Hyper-Spectral Pushbroom (HSP). A comparison between the three separate data acquisition methods that defined the design of each instrument configuration is shown in Figure 1; these are discussed in greater detail in the following sub-sections. Note that for these studies, the Main Electronics Box (MEB) was assumed to reside on the spacecraft and have its thermal control managed separately from the instrument via its own dedicated radiator. Therefore, its dissipations and radiator sizes were not considered in these early design comparisons.

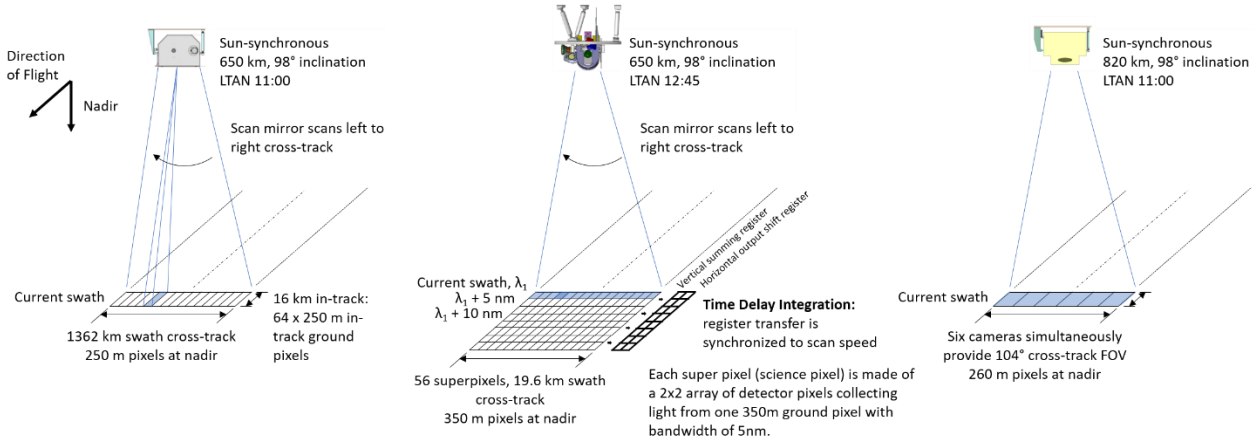

(a) Multi-Band Scanner (MBS) **(b) Hyper-Spectral Scanner (HSS)** **(c) Hyper-Spectral Pushbroom (HSP)**

Figure 1. OCI Instrument Design Configurations Considered in the IDL.

A. Multi-Band Scanner (MBS)

The Multi-Band Scanner was a whisk-broom design with a Rotating Telescope Assembly (RTA), which continuously rotated a scan mirror at 0.4 Hz through a cross-track scan to acquire an image on the ground. The rotating telescope assembly transformed the 112° cross-track field of view into an image that emerged from the side of the RTA housing at a large angle off the rotation axis. The Half Angle Mirror (HAM) spun at half the RTA rate and was located inside the Outboard Spin Bearing, opposite the RTA's drive motor. The center image in Figure 2 shows the optical path at the heart of the MBS configuration, where the signal from the instrument's nadir view is transported via telescope lenses in the spinning RTA to the centrally located HAM, then distributed to three separate downstream channels: a UVVIS channel sensitive between 350 and 580 nm, a VISNIR channel sensitive between 610 and 940 nm, and a SWIR channel sensitive between 1240 and 2250 nm, each with separate detector assemblies.

Two cases were studied: one design which produced 250 m ground sample distance pixels at nadir, and one which produced 500 m. As seen from Figure 2, the RTA was centrally located within the instrument housing, and as it rotated it scanned through views of the Earth via the opened Earth Aperture Door, the Sun via the Solar Aperture, and cold space via the Deep Space Aperture. Protruding from the anti-ram side of the instrument was a housing which protected all three detector assemblies and their respective optics from the harsh space environment. The UVVIS and VISNIR channel detectors were required to be held at -23°C ± 0.1°C to achieve ample radiometric signal, and dissipate 0.6 W

and 0.3 W respectively in the 250 m case, and 0.42 and 0.21 W respectively in the 500 m case. The SWIR channel had a temperature requirement of -93°C ±0.1°C, and dissipated 0.39 W with 250 m and 0.3 W with 500 m. The SWIR and visible channels were read through a single Front End Electronics (FEE) box close by, which output 8.2 W of heat at 250 m, and 4.1 W at 500 m.

Thermal control of the MBS configuration was fairly simple and was achieved with passive heat transport to three dedicated radiators with a view to deep space. The SWIR detector was heat-strapped to an ethane heat pipe and its heat was transported to a SWIR radiator; the UVVIS and VISNIR channel detectors were both heat-strapped to a single ammonia heat pipe which transported to a dedicated visible radiator; heat from the FEE and RTA motors were pulled via dual ammonia heat pipes to an "Instrument Enclosure" radiator. An earth shield covering the SWIR and visible radiators allowed them to passively cool to desired sink temperatures. Precision control on detectors was achieved by cold biasing the detector assemblies and using trim heaters to achieve ± 0.1°C stability. This entire assembly was mounted onto a cruciform flexure at one end and a bipod at the other, connecting it to its instrument baseplate. A tilt motor mounted on the cruciform side allowed the instrument to pitch ±20° to avoid glint.

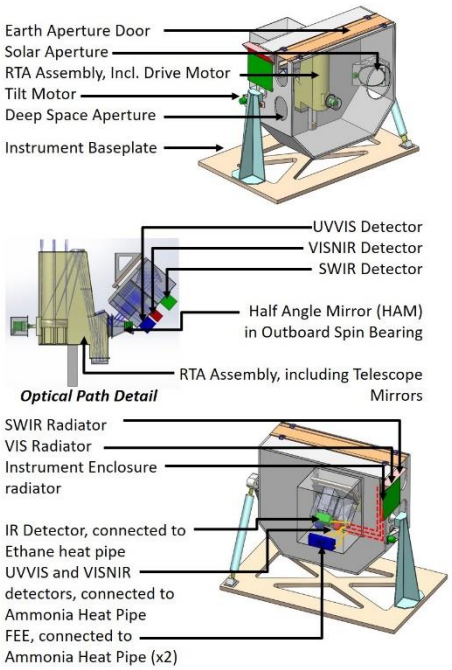

Figure 2. The Multi-Band Scanner.

B. Hyper-Spectral Scanner (HSS)

Similar to the MBS, the Hyper-Spectral Scanner design also employed an RTA, rotating the scan mirror at 18 Hz to acquire the image through a large 120° cross-track Field of View (FOV). The image that emerged from the RTA was transferred via the optical path through the HAM and split into three major wavelength bands: the UVVIS channel between 350 and 555 nm, VISNIR channel between 583 and 865 nm, and six SWIR channels between 940 and 2250 nm. The rotating telescope moved the image of the science pixels across the ground to cover the full field of regard without any gaps in coverage per scan. Then, the detector used Time Delay Integration (TDI)[4] to transfer the charge from pixel-to-pixel at the same rate as the rotating telescope, allowing the same scene to be imaged on the detector for an extended time and building up enough signal to meet signal-to-noise ratio.

Two cases were studied: one design which produced 350m ground sample distance pixels at nadir, and one which produced 500m. Figure 3 speaks to the instrument design: the RTA sat at the heart of the instrument, spun by a motor which contains a counter-rotating component for momentum compensation. The HAM and its rotation mechanism resided diametrically opposite of the RTA motor, and the UVVIS and VISNIR channel detector subassemblies sat immediately downstream of the HAM. Both UVVIS and VISNIR channel detectors were required to be held at -20°C ±0.1°C and dissipate 0.5 W each. Below the rotating telescope, the six SWIR detectors were required to be held at -93°C ± 0.1°C and dissipate a total of about 0.2 W. The FEEs were within close proximity to the detectors; in the 350 m case there is one FEE for the SWIR detectors dissipating 18 W and another FEE for the visible detectors dissipating 22.3 W, while for the 500 m case these electronics were consolidated into one FEE box dissipating 25.5 W. The smaller dissipation in the 500m case was a result of a smaller detector used in the 500 m configuration, reducing the necessary number of FEE cards for readout. The optical telescope, detectors, calibration assembly, and FEEs all sat atop a mechanism which allowed pivoting of the instrument ±20°, supported by the instrument deck structure. Three bipod assembles tied the instrument deck to the spacecraft.

For thermal management of the system, two large radiators were part of the pivoting assembly: the detector radiator and the FEE radiator. The SWIR detector assemblies each siphoned their heat via Ethane Constant Conductance Heat Pipes (CCHP) to a cold plate actively controlled to colder than –93°C by thermoelectric coolers (TEC). Those TECs then rejected their waste heat directly to the detector radiator. The visible detectors each had their own respective high-purity Aluminum heat straps to reject their heat to the same white paint-coated radiator. The FEEs transported their heat through ammonia CCHPs to a dedicated FEE radiator, which itself had embedded ammonia heat pipe

spreaders. A Multi-Layer Insulation (MLI) skirt which is not shown in Figure 3 wrapped around the exterior of the bi-pod assemblies, reducing radiative parasitics to the detector assemblies and cold plate.

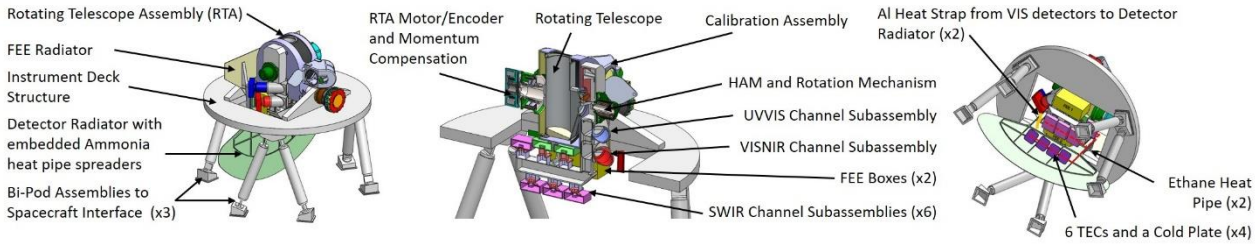

Figure 3. The Hyper-Spectral Scanner Design.

C. Hyper-Spectral Pushbroom (HSP)

The Hyper-Spectral Pushbroom design expanded on the Copernicus program's Sentinel-3 Ocean and Land Colour Instrument (OLCI)[5,6] and the European Space Agency's Medium Resolution Imaging Spectrometer (MERIS)[7] ocean color instrument heritage, taking data across 490 spectral pixels between 342.5 nm and 955 nm, with the additional inclusion of two near-infrared atmospheric correction bands between 820 and 940 nm and five SWIR bands between 1240 and 2250 nm. In the IDL, it was studied in both 260m and 500m spatial resolution configurations. As a "push-broom" design, it relied on simultaneous measurements across a large 104° instantaneous cross-track field of view via the use of six cameras in the 260 m configuration, each covering 17.33° FOV, and five cameras in the 500m configuration, each covering 20.8° FOV. While this eliminated the use of a scan mechanism in the design, it increased the optical and detector readout complexity of the system.

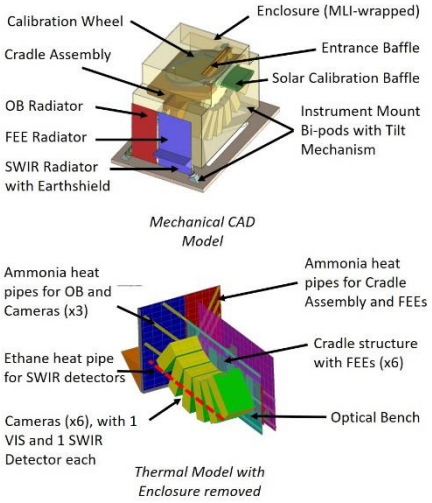

Figure 4. The Hyper-Spectral Pushbroom Design.

As seen from Figure 4, the HSP design consisted of a mechanical cradle assembly which attaches to bi-pods with an integrated tilt mechanism on either end, allowing the instrument itself to pitch ±20°. The cradle assembly contained the calibration wheel with the entrance baffle for the nadir-facing Earth Science signal and the solar calibration baffle, as well as the six FEE boxes. The FEEs were required to be kept below 40°C operational temperatures; there were three visible readout FEEs dissipating 5.8 W each at 260 m and 4.2 W at 500 m, and three SWIR readout FEEs dissipating 3 W each at 260 m and 2.5 W each at 500 m. The OB was mounted atop the cradle structure via flexures, and six cameras (five for 500 m) are aligned precisely on top of the optical bench. Within each camera resided one SWIR detector, one visible detector which covered the full range of UVVIS and VISNIR measurements, and the respective optical elements to shape the image and direct the incoming signal. Each SWIR detector was required to be held at < -123°C ± 0.1°C and dissipated 0.055 W in the 260 m case and 0.045 W in the 500 m case. The operational temperature requirement for each visible detector was < -25°C ±0.1°C and dissipated 1.0 W in the 260 m case and 0.58 W in the 500 m case. An MLI-wrapped mechanical enclosure protected this assembly, and external features on this enclosure included the OB, FEE, and SWIR radiators. The SWIR radiator itself had an earth shield with Silver Teflon exterior and Vapor-Deposited Aluminum (VDA) interior to passively cool to the temperatures required for providing a heat sink to the SWIR detectors.

The thermal control scheme developed for the HSP configuration relied primarily on passive heat management. Manganin wire and long harness lengths were used to minimize the conductive parasitics to the SWIR detector within each camera, and all of the SWIR detectors spread across camera assemblies were tied to an ethane heat pipe, which transferred the dissipations and parasitic heat to the dedicated SWIR radiator. Three parallel ammonia heat pipes pulled heat from the OB and the visible detectors to the OB radiator. Three other parallel ammonia heat pipes connected the cradle assembly and the FEEs to the FEE radiator. The radiators were 0.1 in. (0.254 cm) thick Aluminum

with an AZ93 white paint coating on the space-facing side and MLI on the back side, and contained Proportional-Integral-Derivative (PID) control heaters for tight thermal stability control. There were thermostatically controlled survival heaters for the OB, the FEE radiator, and visible detectors. In the 500 m design, the only significant difference was that the OB and FEE radiators have been combined into one common radiator.

D. Comparison of Thermal Designs

The predictions of heater powers and radiator areas for all three studied configurations are shown in **Error! Reference source not found.**. Power estimates for the instrument MEB were not included in the "Total Instrument Electronics and Mechanisms Dissipations" row within this table, as the MEB was intended to be spacecraft-mounted and its thermal management performed by the spacecraft. Upon cursory observation of the table, a few items immediately become apparent: the HSS family of instruments had an overall smaller mass and volumetric footprint than the MBS or HSP families. While the HSP 500 m configuration did overall have the lowest mass and volume among all the studied cases due to the reduction in number of cameras needed as well as the reduction in optics size with coarser ground resolution, this low-cost solution offered a degraded science product.

Table 1. Comparison of Key Parameters for OCI Designs in the IDL

		Multi-Band Scanner (MBS)		Hyper-Spectral Scanner (HSS)		Hyper-Spectral Pushbroom (HSP)	
Spatial Resolution		250 m	500 m	350 m	500 m	260 m	500 m
Mass of Instrument (kg)		284.6	279	141.5	143.1	203.1	120.5
Volume of Instrument (mm x mm x mm)		2560 x 1600 x 1631	2560 x 1600 x 578	1200 x 1200 x 1161	1200 x 1200 x 1161	1829 x 1219 x 1232	1295 x 762 x 990
Total SWIR Detector Dissipations (W)		0.39	0.3	0.20	0.20	0.33	0.23
Total Visible Detector Dissipations (W)	UVVIS	0.6	0.42	0.50	0.50	6.0	2.9
	VISNIR	0.3	0.21	0.50	0.50		
IR Detector Op Temp Requirement (°C)		-93 ± 0.1	-93 ± 0.1	< -93 ± 0.1	< -93 ± 0.1	< -123 ± 0.1	< -123 ± 0.1
Visible Detector Op Temp Requirement (°C)		-23 ± 0.1	-23 ± 0.1	-20 ± 0.1	-20 ± 0.1	< -25 ± 0.1	< -25 ± 0.1
Total FEE and Mechanisms Dissipations (W)		19.4	15.3	60.7	51.9	32.4	23.0
SWIR Radiator Size (sq. m)		0.169	0.164	0.30	0.30	0.10	0.10
Visible radiator size (sq. m.)		0.042	0.039	--	--	0.33	0.32
FEE Radiator Size (sq. m.)		0.217	0.217	0.18	0.12	0.25	0.25
Oper. Heater Power (W)		7.0	7.0	29.2	29.2	15.0	15.0

For heat dissipations on the instrument, the SWIR detector dissipations were comparable between all configurations. For the visible detectors, the HSP design required a Charge Coupled Device (CCD) with a much larger active area driving its dissipations to be an order of magnitude higher than its counterparts on the MBS and HSS designs, which both employed active scan mechanisms. Regarding electronics and mechanisms dissipations, a combination of greater complexity in the FEE as well as more power-hungry constantly-actuating mechanisms in HSS resulted in a higher dissipation than HSP or MBS.

On the thermal design side, each instrument required a separate SWIR radiator for the cryogenic SWIR detector, and a FEE radiator for the room-temperature components. MBS and HSP had separate visible radiators, as the sink temperature for the visible detectors in these configurations were different than those needed for the FEEs or other instrument components. In the HSS configuration, the visible detector heat was transported to the FEE radiator. Regarding radiator sizes, HSS had a larger detector radiator due to its non-optimal placement encircled within the instrument deck, where it had a view to and backloading from the bipods to the spacecraft. The HSS detector radiator also needed to manage the heat dissipations from the TECs, which were significant – up to 20 W total. The visible radiator area on HSP was significantly larger than HSS or MBS due to the large dissipations from its visible detectors and the long transport distance to the radiator. Pivoting to heater powers, the operational heater powers on HSS were

the highest due to the large radiators and large radiative heat loss from the nadir aperture, which required more heater power in the cold case. Although HSP had large radiators as well, the high dissipations from the visible detector, the large thermal mass, and the relative isolation of the cameras within the housing reduced the need for make-up heat via operational heaters.

E. Selection of Flight Configuration and Evolution of Instrument Architecture to System Requirements Review

The previous section detailed a comparison of thermal designs, which showed significant differences between all configurations considered as well as the strengths and shortcomings of each. Although engineering concerns weighed heavily in determining the design to proceed forward with development for flight, the quality of science data that could be achieved was the ultimate factor in choosing for the flight configuration.

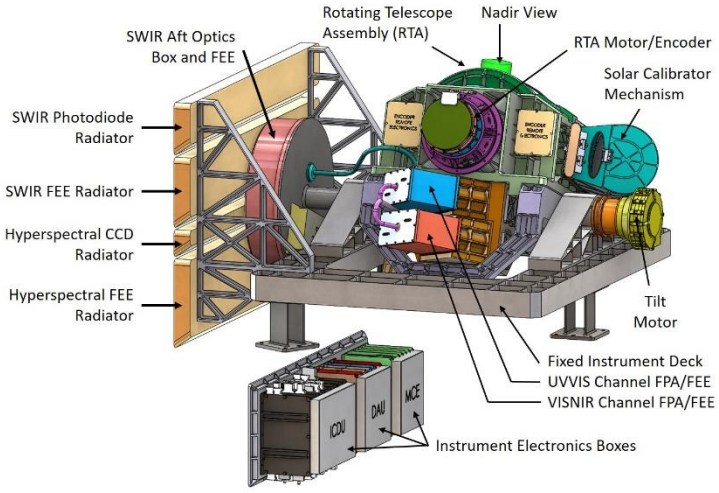

Figure 5. OCI Design at SRR.

From radiometric analysis of each configuration, HSP, MBS, and HSS were all able to achieve sufficient science signal at their detector. However, the HSP concept, being a pushbroom, was susceptible to image striping, increasing the temporal and spatial variability and reducing the accuracy of the science products. A pushbroom concept also required complex pitch and yaw maneuvers to perform lunar calibration, increasing the scientific and technical risk of this monthly calibration. The MBS concept did not meet its Level 1 science objectives either, as the resolution achievable in its data product was 10 nm, versus a 5 nm required resolution for hyper-spectral capability. Its technical implementation was also very difficult, requiring custom detector development. HSS allowed all Level 1 science objectives to be achieved while showing the greatest technical feasibility and lowest risk, and was therefore selected as the best option to proceed forward for flight design.

Advancing towards Mission Concept Review (MCR), a further trade study was performed on the ground sample distance range for HSS, between 500 m and 1000 m spatial resolution. As OCI was cost-constrained, the 1000 m resolution presented a lower cost estimate while still achieving all Level 1 science objectives, and was chosen over the 500 m spatial resolution design to advance to System Requirements Review (SRR). A Solar Calibration Assembly (SCA) containing solar diffusers was also added to monitor the short-term changes in detector response, along with dark blackbody targets at the point of rotation where the telescope views the inside of the RTA housing, to allow for dark current calibration.

The instrument design at SRR is shown in Figure 5. There were some major changes with respect to the original studied HSS configuration: of immediate note is the fixed series of SWIR and visible CCD radiators as compared to the tilting radiators in HSS. To achieve fixed radiators while still allowing for instrument ±20° tilt, the SWIR signal was fiber-coupled out from the RTA to a fixed SWIR Aft Optics Box and FEE, mounted on the radiator. Within the SWIR Aft Optics Box, the optical fibers transmitted the signal to an array of FPAs with photodiodes held at -65°C, each receiving a different wavelength. For subsequent iterations of the SWIR assembly towards the final flight design, this became the SWIR Detector Assembly (SDA), which consisted of the Collimator Slit Assembly (CSA) and the Aft Optics Bench (AOB). For the UVVIS and VISNIR assemblies, the CCD and FEE were both held at -30°C and rejected their heat through flexible thermal straps to the fixed hyper-spectral radiators. Heat dissipated by the RTA motor and HAM motor were sunk into the RTA structure and managed passively. The electronics boxes were now

divided from one MEB to the Instrument Command and Data Unit (ICDU), the Data Acquisition Unit (DAU), and the Mechanism Control Electronics (MCE), and their heat dissipations were managed by the spacecraft.

Component	HSS (500 m)	SRR	PDR	CDR	TV
Mass of Instrument (kg)	143.1	190	246	263	266
RTA Rotation Speed (Hz)	18	6	6	6	6
UVVIS Detector + FEE Dissipations (W)	2.6	15.4	12.9	11.2	10.6
VISNIR Detector + FEE Dissipations (W)	2.6	15.4	12.9	11.2	10.6
SWIR Detectors + FEE Dissipations (W)	12.9	20.0	10.0	5.4	5.4
UVVIS Radiator Size (m^2)	--	0.15	0.18	0.22	0.22
VISNIR Radiator Size (m^2)	--	0.15	0.18	0.22	0.22
DAU Radiator Size (m^2)	--	0.38	0.27	0.30	0.30
ICDU Radiator Size (m^2)	--	0.16	0.09	0.17	0.17
MCE Radiator Size (m^2)	--	0.16	0.09	0.09	0.09
RT Radiator Size (m^2)	--	--	0.12	0.03	0.03
HAM Radiator Size (m^2)	--	--	0.12	0.03	0.03
SDA (CSA + AOB) Radiator Size (m^2)	0.3	0.39	0.40	0.45	0.45
Operational Heater Power (W)	29.2	57.6	69.2	50.0	50.0

shows the updated values for SRR for heater powers and radiator areas and compares them with the studied HSS 500 m spatial resolution configuration, as well as the Preliminary Design Review (PDR), Critical Design Review (CDR), and more recent post-Thermal Vacuum (TV) configurations.

Table 2. Comparison of Key Thermal Parameters for the HSS 500 m Study, SRR, PDR, CDR, and Current TV OCI Configurations.

Component	HSS (500 m)	SRR	PDR	CDR	TV
Mass of Instrument (kg)	143.1	190	246	263	266
RTA Rotation Speed (Hz)	18	6	6	6	6
UVVIS Detector + FEE Dissipations (W)	2.6	15.4	12.9	11.2	10.6
VISNIR Detector + FEE Dissipations (W)	2.6	15.4	12.9	11.2	10.6
SWIR Detectors + FEE Dissipations (W)	12.9	20.0	10.0	5.4	5.4
UVVIS Radiator Size (m^2)	--	0.15	0.18	0.22	0.22
VISNIR Radiator Size (m^2)	--	0.15	0.18	0.22	0.22
DAU Radiator Size (m^2)	--	0.38	0.27	0.30	0.30
ICDU Radiator Size (m^2)	--	0.16	0.09	0.17	0.17
MCE Radiator Size (m^2)	--	0.16	0.09	0.09	0.09
RT Radiator Size (m^2)	--	--	0.12	0.03	0.03
HAM Radiator Size (m^2)	--	--	0.12	0.03	0.03
SDA (CSA + AOB) Radiator Size (m^2)	0.3	0.39	0.40	0.45	0.45
Operational Heater Power (W)	29.2	57.6	69.2	50.0	50.0

III. OCI Flight Design

Moving beyond SRR, the OCI thermal design experienced a few more refinements as the instrument made its way into PDR, CDR and Flight TV design. The flight thermal design is generalized in the block diagram shown in Figure 6. OCI is mostly a passive design with straps and radiators to conduct heat either to the radiators or to space, with the

exception of the FPA thermal control which requires dedicated Loop heat pipes (LHPs). More on the rationale for incorporating LHPs is provided in the following subsections.

The following sections attempt to capture some of the thermal changes of the instrument as it passed through major instrument development phases, as well as some lessons learned along the way. At OCI-level environmental testing, OCI was exposed to Electromagnetic Interference (EMI), Vibration, Acoustics, and Thermal Vacuum Testing. After instrument environmental testing, OCI was then integrated to the spacecraft to become part of the PACE Observatory and exposed to similar environmental testing, following the guidelines and requirements laid out in the General Environmental Verification Standard (GEVS) document.

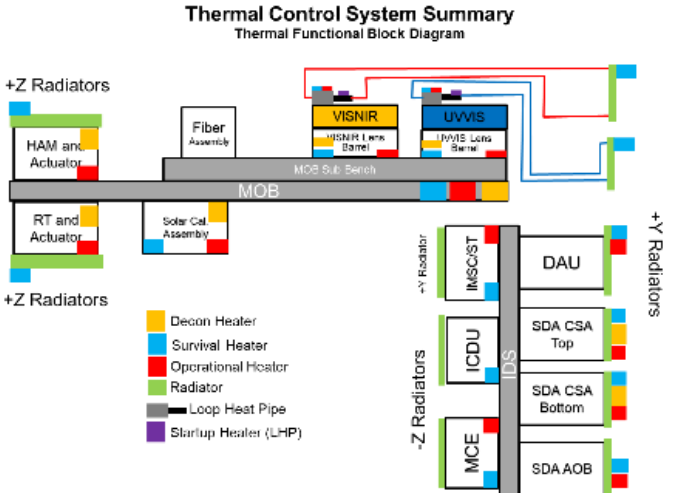

Figure 6. OCI TCS Block Diagram.

A. OCI at Preliminary Design Review (PDR)

At PDR, OCI was more complex from a systems perspective than a thermal perspective. The complexity of OCI at PDR mainly derived from the measurement of critical science wavelengths, while isolating grounding issues from electrical noise sensitive components within the DAU and FPA subsystems. A view of OCI at PDR is shown in Figure 7. Between SRR (review gate pre-PDR) and PDR, the thermal changes to instrument included:

1. The star tracker being moved to OCI
2. The ±20° Tilt actuation being moved out of OCI and becoming part of the Spacecraft entity
3. EMI gaskets being introduced at the FPA/LHP interface
4. The ICDU and MCE being moved from the spacecraft (S/C) to the instrument
5. The stability requirements being introduced which resulted in the addition of a Heater Control Card to the ICDU.

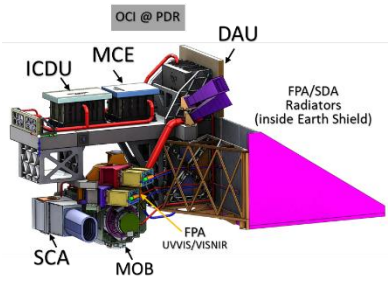

Figure 7. OCI at PDR

The star tracker moving to OCI was a change to provide a better understanding of OCI pointing in relation to the OCI primary mirror bore sight, as all components would be held by the primary structure. With the star tracker on the S/C, the uncertainty would have been too large to accurately calculate whether OCI was pointing directly at Earth. This was verified by performing the Structural, Thermal and Optical (STOp) analysis, performed through following process: 1) the stress analyst provided a meshed model, with data on nodes and location with some reference point to the thermal analyst; 2) the thermal engineer then overlayed the meshed mechanical model over the thermal model; 3) the thermal analyst mapped temperatures to each structural node; 4) the stress analyst received inputs from Optical engineer on the light path of the optical system; 5) the stress analyst combined the structural, thermal and Optical model to produce line of sight error value as well as any point-to-point reference misalignment, such as the star trackers to OCI bore-sight.

The tilt actuation moved from being a part of the instrument to external to the instrument, as a spacecraft-mounted mechanism that cradled OCI. This was driven due to the challenges of having a flexible thermal system to maintain FPA temperatures, which were part of the Optical Module that was originally being tilted within OCI. The choice of having the entire instrument tilt simplified the thermal and mechanical design of the instrument, but did add weight to the observatory as the new tilt interface would be required to carry the mass of the instrument. EMI gaskets were added between the FPA and LHP evaporator interface in support of shielding the FPA CCDs from radiative electrical noise. This approach decreased the radiative susceptibility of the FPAs, but also added an interface that resulted in a temperature delta; this delta was one that thermal had to account for in maintaining CCD temperatures. The ICDU and MCE were moved to the instrument for simplification of the instrument build, but unfortunately added two new thermal control zones to the instrument for operational temperature maintenance. Lastly, one of the major impacts to

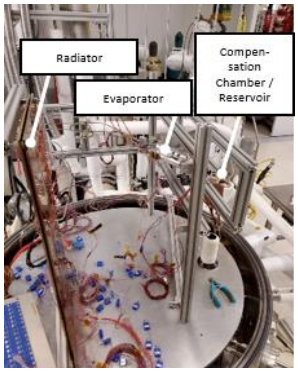

Figure 9. ETU LHP in TV Testing.

thermal was the introduction of new stability requirements. These stability requirements necessitated radiator growth, heater power and an additional card for proportional control. The Optical Module (OM) stability requirement over an orbit changed to ±2.5°C and the FPA CCDs stability was introduced at ±0.5°C over an orbit. With the new stability requirements, the need for additional heater card to operate heaters with a proportional approach vs. ON/OFF was also required, which directly impacted the ICDU total power consumption.

Between SRR and PDR, another major addition to the OCI Thermal Control System (TCS) was LHPs. Loop heat pipes provide a means for transporting heat from source to radiator/condenser through capillary action. Multiple benefits of LHPs proved highly useful on OCI, including transport of heat over long distances and lack of sensitivity to orientation. These LHPs were introduced to provide the least technical impact to mission while also providing adequate thermal control for the FPAs. Given the long (~30 in. / 76 cm) distance of FPAs away from a direct view to space and a need for precise temperature control and mass/power budget, it became evident through thermal trade studies that LHPs would be the best option. Constant conductance heat pipes would have required 60W additional heater power, and would have been extremely sensitive to orientation, as OCI has to go through ±20° tilt operation during ground testing. Thermal straps would have required considerable mass increase (~25 kg) as well as the 60W heater power hit. Though LHPs represented a significant increase to schedule and budget, these considerations reinforced the need for LHPs to provide the best thermal performance for the FPAs. For OCI, Thermacore was chosen as the vendor for the LHPs, with a very robust design to withstand OCI tilt actuation, provide thermal stability and withstand large temperature gradients (up to 100°C between radiator and FPA, during survival mode).

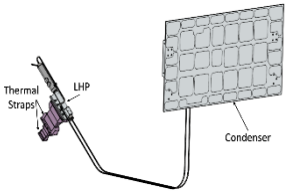

Figure 8. LHP with Thermal Straps.

Moving towards CDR, the instrument incorporated the thermal changes described above. In addition, there was an Engineering Test Unit (ETU) built of the loop heat pipe and FPA Thermal Straps. These ETUs were identified as risk reduction units to verify whether the expected temperature drop, given the dissipation, environment and radiator sizing would provide FPA CCDs with temperature control per requirements; see Figure 8 for the schematic of the LHPs and thermal straps. Testing of ETUs did provide insight into temperature drop across the LHPs from condenser to evaporator as well as the temperature vs. power performance curve for this specific LHP design. Figure 9 shows the setup of the ETU LHP inside the chamber. Although this was not a flight-like or ground-test-like setup, the importance of this test was to ensure there was no gravity influence on the transport lines and that the reservoir was in a non-adverse orientation, and both these requirements were met through this setup. Results from this test showed that, to maintain the FPA CCDs at -25°C (for worst case hot) and -35°C (worst case cold), the radiator sizing would have to increase by approximately 15%.

B. OCI at Critical Design Review (CDR)

At the end of preliminary design phase, the OCI thermal system had changed very little to reflect the outcome from risk reduction testing as well as design iterations. Risk reduction testing was performed on the loop heat pipe and thermal straps, which is briefly discussed in following paragraphs. Some of the design changes leading up to CDR included:

1. Adding mechanism radiators
2. Adding Blanket Support Structure (BSS)
3. Adding a switched survival service for the LHP
4. LHP Radiator growth
5. Increased thermal telemetry during survival mode

Regarding the first change, the addition of mechanism radiators was driven by the desire to not have part of the mechanism housing acting effectively as a radiator. If the mechanism enclosure were to act as a radiator, it would have limited the view to space given the amount of wiring and need for constant access; this could have damaged the coating. Figure 10 shows the view of the optical module with mechanisms/motors attached and radiators mounted. With respect to the second change, the addition of BSS is shown highlighted in blue in Figure 11. The BSS was introduced to provide support for the blankets above the LHPs as well as the Optical module. This change was driven by the need to reduce solar entrapment that would occur in that area during the daylight portion of the orbit.

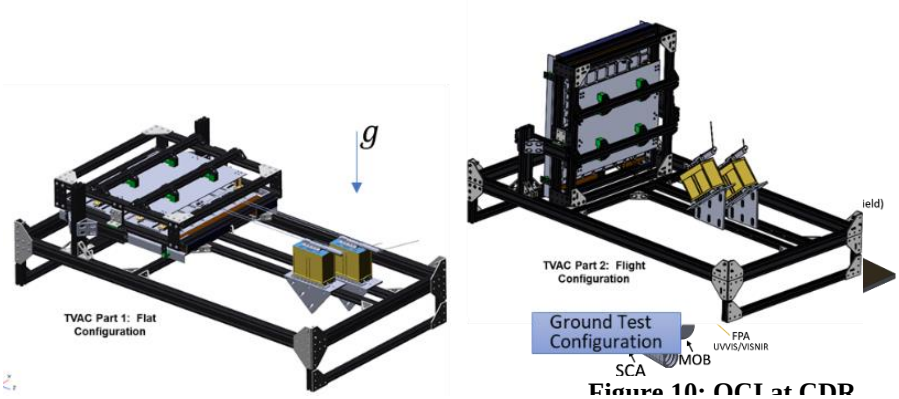

Figure 12: Flight LHP Test Setup.

Change 3 above, to add a switched LHP survival heater service, was due to the need for temperature maintenance during survival mode for the FPAs. With a switched service, there was a software link developed between the FPAs' power service and the LHP's Survival service. This allowed for the LHP Survival service to be disabled every time FPAs were powered ON. Change 4 regarding LHP radiator growth was a result of ETU LHP testing as described in the previous PDR section. Change 5 was to allow for additional temperature monitoring of OCI during survival and safe mode. Typically, it is important to have one sensor for each critical box, subsystem, or component; this allows for temperature data even when the instrument is unpowered. Also, design conventions dictated that any component with a survival heater received a sensor to monitor its temperatures during survival mode. Due to this, the increase in number of thermal sensors was negotiated from four to ten for OCI.

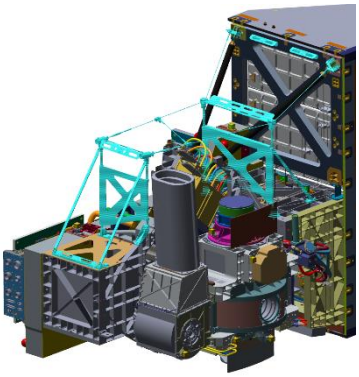

Figure 11: Blanket Support Structure.

The COVID-19 Pandemic placed increased challenges on the procurement of critical hardware. Leading up to the CDR, the main focus for the thermal team was to ensure that the long lead items were put on order. Heaters and blanketing were the major part of thermal subsystem procurement, with the LHP being the other major procurement. Since the design for LHP did not require any change in power or temperature and only required a slight mechanical design change, it was decided to do an upgrade of the ETU LHPs to Flight units. The challenges in upgrading the LHP to flight included re-machining of the FPA thermal interface, and there were some gaps widened to allow for thermal expansion while maintaining the purpose of the features. Also, there was welding of new transport lines to accommodate the shorter length for flight design. These changes were fluidly executed by the LHP vendor, Thermacore.

C. OCI at Thermal Vacuum Test Peer Review

Progressing from CDR to the instrument-level TV and Thermal Balance (TB) tests, one of the major tasks for the thermal subsystem was the verification and readiness of the Flight LHPs. The UVVIS and VISNIR LHPs underwent a gravity neutral configuration test and then a flight-like configuration test. Gravity neutral (flat configuration, as built) indicates when the unit had the least/negligible amount of gravity influence on the transport system. Flight configuration indicates the orientation in which the LHPs would be tested when integrated into OCI. Both of these configurations are shown in Figure 12. Leading up to the start of LHP TV testing, a mockup of the LHP was built to understand the integration challenges at the OCI level; the lessons learned from this mitigated difficulties during the flight integration. One of the major challenges during OCI integration was to maneuver the units with thin transport line tubing and independent movement between pump body and radiator; having a mockup allowed for technicians to practice before the flight unit handling. Another lesson learned through Flight LHP TV testing was to mimic the start-

up of the LHP. Unless planned for, LHPs induce a thermal shock to the attached mass to the evaporator. The potential thermal shock on OCI was a temperature drop from 0°C to -60°C at the evaporator-to-FPA thermal interface. With proper planning and understanding the sequence of OCI power ON, the LHPs were adjusted to alleviate the thermal shock and narrow the range to 0°C and -5°C. Another lesson learned was to have startup heaters with different power; this allowed for choosing makeup heaters that did not adversely impact performance. For OCI, there was a 7 W and a 10 W startup heater. After LHP testing, it was observed that at operational temperatures keeping the 7 W startup heater provided adequate LHP operation, whereas 10 W resulted in slightly warmer CCD temperatures. Overall, the Flight LHP testing was a very successful campaign that verified that the LHPs will be able to maintain the CCD temperatures throughout the protoflight range as well as operational range when exposed to worst case environments.

Late in the design process, the SDA Pulse Calibration Assembly (SPCA) was added as a passive optical pulse generator that was used to calibrate the SDA. From ETU testing of the SDA, it was realized that the detector and FEE response were too slow to match the speed of the rotating telescope, putting Level 1 requirements associated with the SWIR data products at risk. Using the sun, the SPCA created an impulse response used to trend and calibrate the SDA signal over the life of the mission, providing an onboard signal to allow for software correction and on-orbit calibration to achieve requirements.

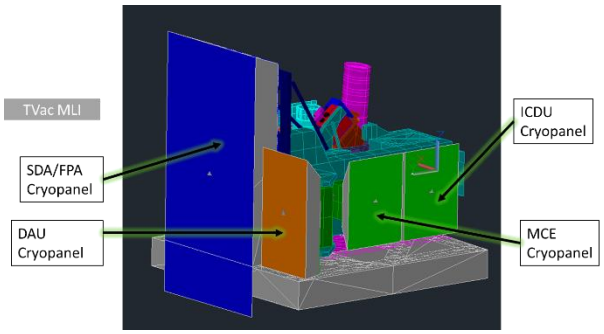

Figure 13: OCI TVAC GSE Setup.

Once the instrument was fully integrated and underwent EMI and Vibration/Acoustics testing, it was then exposed to worst-case on-orbit thermal environments. OCI TV testing was a sixty-day test campaign composed of calibration activities, protoflight level testing, bakeout, survival and operational thermal balances. In order to achieve the goals of the test, a setup was constructed to provide radiative views and similar sink temperatures that each of the following key components would experience on orbit: DAU, MCE, ICDU, FPA/SDA and the Main Optical Bench (MOB). A schematic of the setup is shown in Figure 13. Lessons learned from this test are captured in Section IV.

IV. Instrument Testing Lessons Learned

There were two major lessons learned from this effort; this included:

1. **MOB Heater Control Approach:** During OCI TV test nominal operation temperatures, the science and systems team had observed a cyclical behavior within the signals at 940nm. The MOB HAM heater, along with all of the heaters on the MOB structure were designed with a bang-bang (ON/OFF) software control approach. Even after lowering the deadband, it was realized that the physical limitation of the heater card response had been achieved and no further deadband adjustments would have improved the steady-state oscillations. See Figure 14 for the heater vs. signal response plot. Additionally see Figure 15 for the multiple attempts that were made to achieve a smaller deadband for the MOB HAM Heater, but were not successful.

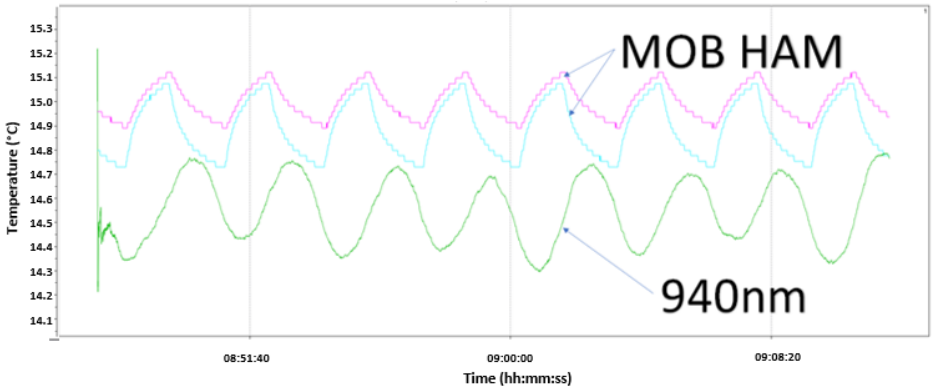

Figure 14: MOB HAM Heater vs. 940nm Signal Response.

Lesson Learned: always utilize a heater control approach that provides thermal stability (±0.5°C over an orbit) for an optical system. For OCI, the requirement on the MOB is ±2.5°C over an orbit. Although this requirement was met analytically and through testing during transient cases, it was observed that this may have been too wide of a deadband range.

Lesson Learned: the MOB was constructed from Aluminum 6061. Using composite or carbon-fiber would have provided much better optical stability due to its much lower coefficient of thermal expansion.

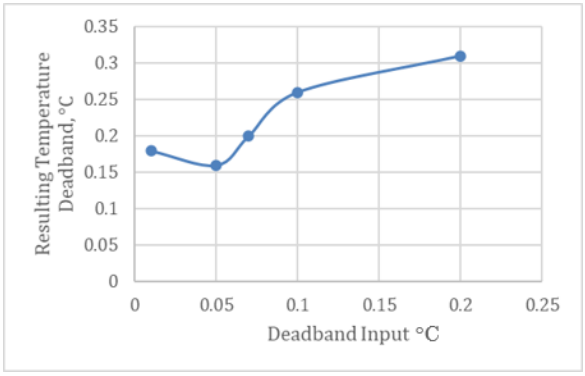

Figure 15: MOB Heater Deadband vs. Output.

2. **LHP Reservoir Shutdown and Operational heater sizing:** During transition to the OCI survival test phase, it was observed that the UVVIS LHP had gone into a self-start situation. Self-start is when LHP achieves the right type of temperature gradients as well as an external influence on system that causes an unexpected start while in shutdown mode. During the transition to survival, the radiator was at -100°C, the reservoir was cycling at 8°C to 15°C and the FPA was at 20°C (due to transitioning from Bakeout temperature of 40°C). As soon as UVVIS LHP self-start occurred, the cold fluid (-100°C) rushed into the reservoir (8°C) and resulted in the FPA CCD temperature to drop at ~3.5°C/min, whereas the requirement was 0.5°C/min. At this point the shutdown heater (~9W) was not sufficient to overcome the self-start. The main driver to this was found to be the additional pressure head from gravity induced on the vertical run of liquid line. Due to the reservoir being lower than the exit of the liquid line from radiator, this resulted in the LHP having to deal with this additional pressure head. On orbit, if a self-start occurs then it is likely going to cause a much less severe temperature drop on FPA CCDs.

Lesson learned: discuss with the instrument/observatory systems team on how the LHP will be utilized for ground testing as well as on orbit operations. This included phases such as survival, cold startup, and any idiosyncrasies to be aware of during protoflight testing. This also helped in sizing the operational heater, as the steady state need was no more than 2W, while the startup needed a full 9.5W of heater power on the reservoir.

V. Conclusion

This paper addressed the overall design process of the OCI instrument on PACE, from trade studies performed within the Instrument Design Laboratory at GSFC all the way to modifications for flight implementation, and lessons learned from flight integration. Figure 16 gives a visual overview of the design changes from MCR to CDR. Although there was a lot of variation and flux in engineering resources between the early designs of OCI, latter iterations, especially from SRR onwards, showed only marginal changes in detector dissipations, radiator sizes, and heater powers. For OCI, the greatest thermal impact occurred with the addition of the instrument electronics boxes to the instrument itself, rather than being mounted to the spacecraft as in earlier design iterations. This drove much of the initial increase in instrument dissipations and radiator sizes from the IDL HSS 500m design to the SRR and PDR design.

With the solidification of the design from SRR to the as-built TV configuration, operational heater powers only decreased by 15%, and total radiator area only increased by 9% over the five-year design period between those two bookend milestones. This speaks to the accuracy in which early design estimates manage to capture the thermal design needs of the instrument, and the confidence in which the thermal designer can provide order-of-magnitude estimates early-on so long as sufficient design margins are held. As usual, the commonly used 30% over Current Best Estimate values from SRR was sufficiently conservative to encompass as-built flight values. Through this comprehensive look at OCI's thermal control architecture evolution, the engineering drivers that have shaped it, and the design

modifications that were driven by project decisions at each milestone and through the integration and testing process, it is hoped that OCI's experience will help inform and advance future instrument thermal designs to anticipate trends spanning the full instrument development timeline.

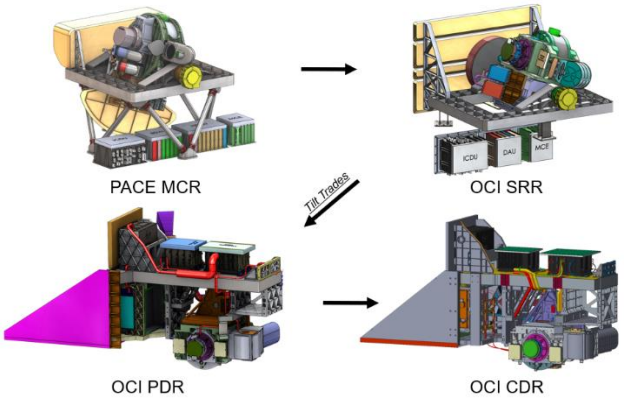

Figure 16. Overview of OCI Design Changes from MCR to CDR.

Acknowledgments

The authors would like to thank: Sergey Semenov and Triem Hoang for their expertise on LHP as well as on-demand analysis for any issues that were observed throughout instrument and component level testing; Chris Stull for his extensive support on FPA development and testing as well as leading the LHP test and correction of the LHP temperature control algorithm; Colin Adamson for leading instrument level analysis and Thermal Vacuum configuration development.

References

[1]Barnes, R., Holmes, A. "Overview of the SeaWiFS ocean sensor." *Proceedings Sensor Systems for the Early Earth Observing System Platforms*, Proceedings Vol. 1939, Orlando, FL, 1993.

[2]Pagano, T., Durham, R. "Moderate Resolution Imaging Spectroradiometer (MODIS)," *Sensor Systems for the Early Earth Observing System Platforms*, Proceedings Vol. 1939, Orlando, FL, 1993.

[3]Ardanuy, P., et al. "NPOESS VIIRS design process," *Earth Observing Systems VI*, Proceedings Vol. 4483, San Diego CA, 2001.

[4]McIntire, J., Kitchen-McKinley, S., Choi, H., Meister, G. "Progressive TDI Measurements with the PACE OCI ETU." *Proceedings of SPIE*, Vol. 11829, 2021.

[5]Nieke, J., Borde, F., Mavrocordatos, C., Berruti, B., Delclaud, Y., Riti, J. B., Garnier, T. "The Ocean and Land Colour Imager (OLCI) for the Sentinel 3 GMES Mission: status and first test results"", *Proceedings of SPIE* Vol. 8528, Earth Observing Missions and Sensors: Development, Implementation, and Characterization II, 85280C, 2012

[6]De Stefanis, M., Melendo, I., Cluzet, G., Dolce, S. "Sentinel 3 – Spacecraft Thermal Control: design, analysis and verification approach." *45th International Conference on Environmental Systems*, ICES-2015-19, Bellevue, Washington, 12-16 July, 2015.

[7]Rast, M., Bezy, J. L., Bruzzi, S. "The ESA Medium Resolution Imaging Spectrometer MERIS a review of the instrument and its mission." *International Journal of Remote Sensing*, Vol. 20, Issue 9, pp. 1681-1702, 2010.